J. Fluid Mech. (1985), *vol.* 157, *pp.* 265–287
Printed in Great Britain

Inviscid compressible flow with shock in two-dimensional slender nozzles

By C. Q. LIN
Northwestern Polytechnical University, Xi'an, Shaanxi 710036, China

AND S. F. SHEN
Sibley School of Mechanical and Aerospace Engineering, Cornell University, Ithaca, New York 14853

(Received 16 January 1984 and in revised form 14 December 1984)

The present theory provides an asymptotic-expansion method for inviscid compressible flows with shock in arbitrary two-dimensional slender nozzles. The flow in front of the shock is assumed to be potential, whereas the flow behind the shock is considered to be rotational owing to the presence of the shock. A parameter that measures the slenderness of the nozzle is used as the expansion quantity. It is found that, except for the region immediately behind the shock, the same coordinate scale can be used for the flows both in front of and further downstream behind the shock. The flows for the regions thus obtained show that all the streamlines are approximately affinely similar to the nozzle wall, and the leading term of the transverse pressure gradient is determined by the local wall shape. For the flow region immediately behind the shock, however, the transverse pressure gradient just behind the shock is determined by the shock conditions rather than by the local wall shape, and a solution is found for that region which transforms the transverse pressure gradient from that determined by the shock conditions to that determined by the local wall shape. The well-known flow singularity at the intersection of the wall and the shock is involved in the solution. Meanwhile, a critical shock location at which the flow has no singularity is derived. A numerical example shows also that the inviscid flow may separate from the wall, owing to the different entropy increase across the shock for different streamlines. The predicted separation point, however, is only of qualitative value, since our theory does not account for reverse flows.

1. Introduction

Much research has been devoted to analytical solutions of the compressible nozzle-flow problem, and in the present paper we are mainly concerned with the presence of the shock in the flow. It is believed that such a solution is valuable both for basic understanding of the flow phenomena and as a check of various numerical methods based upon discretization. In Lin & Shen (1981) a simple example of transonic flow with shock in two-dimensional slender nozzles was given. The entropy increase across the shock was neglected, and the small-perturbation potential equation for transonic flow was used for both the flows before and behind the shock. A well-known exact solution of small perturbation was used for the flow before the shock, and the shock shape was assumed to be a parabola somewhere in the nozzle. By using a series-expansion method, the flow field, as well as the nozzle wall, behind the shock was evaluated to fit the shock conditions. The curvature of the nozzle wall

at the shock point thus obtained is discontinuous. This result is a manifestation of the well-known fact that continuous curvature of the wall at a shock point generally demands singular local behaviour of the flow and the shock shape.

For slender smooth nozzles of hyperbolic shape a complete treatment using the asymptotic-expansion technique and including numerical examples was subsequently presented in Lin & Shen (1982). Though independently worked out, both the basic idea of an inner region immediately behind the shock and much of the analytical development were found to be closely parallel to the earlier work of Messiter & Adamson (1975). In fact, extensions of the same idea had appeared already in the treatment of unsteady transonic channel flows with shock (Richey & Adamson 1976; Chan & Adamson 1978; Adamson, Messiter & Liou 1978). Nevertheless, Lin & Shen (1982) does contain important additional results, such as the alternative formulations of velocity potential and stream function, and one more higher-order term in the expansion expressions for each dependent variable. The entropy rise thus makes its appearance. Of even more practical interest is that the theory is carried through to provide numerical examples, which quantitatively compare the predictions of the alternative formulations, in both two-dimensional and axisymmetric cases, as well as with the results from a state-of-the-art finite-difference computation.

The present research is an extension of the theories of Messiter & Adamson (1975) and Lin & Shen (1982), which were limited to the transonic range, to include flows from low subsonic to supersonic. The inviscid compressible flow with shock in slender two-dimensional nozzles of arbitrary shape is again analysed using the asymptotic-expansion method. The leading terms of the expansions are assumed to be the local one-dimensional solution, instead of the sonic state as in the earlier papers. As the shock strength is not necessarily weak, the vorticity behind the shock can no longer be neglected, and the inviscid Euler equations should be used in this region. The slenderness of the nozzles implies that the variation of any flow parameter along the axial direction is, generally, smaller in order than that along the transverse direction. As in boundary-layer theory, the governing equations, which are elliptic in the subsonic region and hyperbolic in the supersonic region, are thus reduced to parabolic type, and the successive expansion terms are easy to solve. All the streamlines are found to be approximately affinely similar in shape with the nozzle wall (i.e. each streamline is approximately given by the locus of points at the same transverse coordinate when normalized by the local gap width), and the variation of the transverse pressure gradient is determined by the local wall geometry (gap width, slope and curvature). These features are quantitatively discussed in §3. For convenience, *we call this kind of flow the smooth flow in the present paper*. In the regions in front of the shock and further downstream behind the shock, the flow is usually smooth. Immediately behind the shock, however, the transverse pressure gradient is determined by the shock conditions instead. Therefore immediately behind the shock there is usually a short transition region in which the transverse pressure gradient changes from that determined by the shock conditions to that determined by the local wall shape. This short transition region disappears only if the two transverse pressure gradients coincide. We shall discuss this condition in §4.

Thus the flow field is divided into three parts: the smooth region in front of the shock, the short transition region behind the shock and the smooth flow region further downstream behind the shock. In the following the latter two are referred to respectively as the inner region and the outer region behind the shock.

Computation has been carried out for a hyperbolic nozzle as the shock is made to

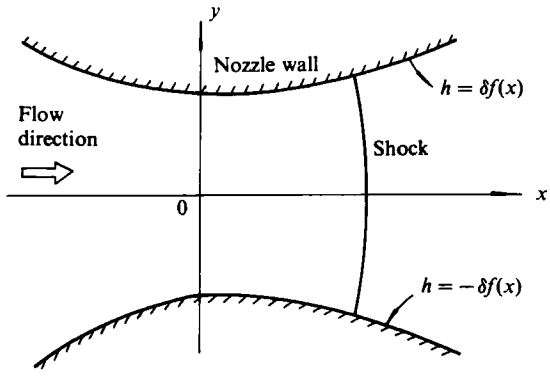

FIGURE 1. Coordinates and geometry of the nozzle.

occur further and further downstream and become stronger. A systematic evolution of the shock shape is revealed. In a separate numerical example, evidence is also found for the phenomenon of shock-induced inviscid separation. Imagine a rather strong shock occurring somewhere across the nozzle section with larger entropy increase near the wall than that near the axis. In this case the total mechanical energy near the wall is lower than that near the axis. If the flow behind the shock is further decelerated, the flow near the wall may lose all its kinetic energy while the flow near the axis still moves forward. Local reverse flow may develop. Not unlike a viscous boundary layer, under an adverse pressure gradient the inviscid flow would separate from the nozzle wall. Systematic analysis of this phenomenon has not been attempted.

2. Coordinate system

Consider two-dimensional compressible flow in a slender symmetric converging–diverging nozzle of arbitrary shape. The Cartesian coordinate system is shown in figure 1. The x-axis is along the line of symmetry and pointing downstream, the y-axis is in the transverse direction, and the origin 0 is placed at the throat section. The equation of the nozzle wall is assumed to be

$$h = \pm \delta f(x), \tag{1}$$

where h is the half-height of the nozzle, $f(x)$ is an arbitrary smooth function of x, and $\delta (\ll 1)$ is a slenderness parameter. We can take $f(0) = 1$ at the throat without loss of generality. It is noted that (1) is essentially different from the slender-nozzle wall equation in the earlier papers of Messiter & Adamson (1975) and Lin & Shen (1982), where the form of $h = \pm(1+\delta f(x))$ was used. Therefore, in the latter case, the nozzle becomes a channel of constant cross-section as $\delta \to 0$, so that the leading term of the asymptotic expansion was taken to be the uniform state, i.e. the sonic state in the previous papers, and only the transonic flow was considered there. In the present paper, however, (1) shows that the relative variation of the cross-section remains unchanged as $\delta \to 0$ so as to include the wider flow range from low subsonic to supersonic.

A curvilinear coordinate system (ξ, η) defined by

$$x = \xi, \quad y = \delta f(x)\,\eta \tag{2}$$

is next taken, with $\eta = 0$ corresponding to the nozzle axis and $\eta = \pm 1$ to the nozzle walls. In tensor notation the coordinates (ξ, η) can be expressed as

$$\xi = x^1, \quad \eta = x^2, \tag{3}$$

and the covariant components of the metric tensor defined by

$$ds^2 = dx^2 + dy^2 = g_{ij}\, dx^i\, dx^j \tag{4}$$

are obtained as

$$g_{11} = 1 + \delta^2 f'^2 \eta^2, \quad g_{12} = \delta^2 f f' \eta, \quad g_{22} = \delta^2 f^2. \tag{5}$$

Note that the summation convention is applied in (4) and also later in the present paper. The contravariant components of the metric tensor can also be evaluated by

$$g^{11} = \frac{g_{22}}{g}, \quad g^{12} = -\frac{g_{12}}{g}, \quad g^{22} = \frac{g_{11}}{g}, \tag{6}$$

where

$$g = g_{11} g_{22} - g_{12}^2. \tag{7}$$

Substituting (5) into (7) and (6), we have

$$g = \delta^2 f^2, \tag{8}$$

and

$$g^{11} = 1, \quad g^{12} = -\frac{f'}{f}\eta, \quad g^{22} = \frac{1}{\delta^2 f^2}(1 + \delta^2 f'^2 \eta^2). \tag{9}$$

It is known that any vector $\boldsymbol{A}$ can be determined by its covariant components (A_1, A_2) or its contravariant components (A^1, A^2) as

$$\boldsymbol{A} = A^k \boldsymbol{e}_k = A_k \boldsymbol{e}^k, \tag{10}$$

where

$$\boldsymbol{e}_k = \frac{\partial x}{\partial x^k}\boldsymbol{i} + \frac{\partial y}{\partial x^k}\boldsymbol{j}, \quad \boldsymbol{e}^k = \frac{\partial x^k}{\partial x}\boldsymbol{i} + \frac{\partial x^k}{\partial y}\boldsymbol{j}, \tag{11}$$

and $\boldsymbol{i}$ and $\boldsymbol{j}$ are the unit vectors of Cartesian coordinates. Then the covariant differentiations of the contravariant components can be expressed as

$$\left.\begin{aligned} A^1_{,1} &= \frac{\partial A^1}{\partial \xi}, \quad A^1_{,2} = \frac{\partial A^1}{\partial \eta}, \\ A^2_{,1} &= \frac{\partial A^2}{\partial \xi} + \frac{f''}{f}\eta A^1 + \frac{f'}{f}A^2, \quad A^2_{,2} = \frac{\partial A^2}{\partial \eta} + \frac{f'}{f}A^1. \end{aligned}\right\} \tag{12}$$

3. Solutions in front of the shock and further downstream of the shock

We shall consider inviscid flow of a perfect gas with constant specific heats. With $\mathscr{U}^1$, $\mathscr{U}^2$, ρ and p denoting the contravariant velocity components, density and pressure respectively, the governing equations for the flow are the equation of continuity

$$(\rho \mathscr{U}^1)_{,1} + (\rho \mathscr{U}^2)_{,2} = 0, \tag{13}$$

the x-momentum equation

$$\rho \mathscr{U}^1 \mathscr{U}^1_{,1} + \rho \mathscr{U}^2 \mathscr{U}^1_{,2} = -g^{11} p_{,1} - g^{12} p_{,2}, \tag{14}$$

the y-momentum equation

$$\rho \mathscr{U}^1 \mathscr{U}^2_{,1} + \rho \mathscr{U}^2 \mathscr{U}^2_{,2} = -g^{12} p_{,1} - g^{22} p_{,2}, \tag{15}$$

and the equation of constant entropy along the streamlines

$$\mathscr{U}^1\left(\frac{p}{\rho^\gamma}\right)_{,1}+\mathscr{U}^2\left(\frac{p}{\rho^\gamma}\right)_{,2}=0, \tag{16}$$

where γ is the ratio of specific heats of the gas. All the velocity components, densities and pressures are non-dimensionalized with respect to the critical speed V_*, critical density before the shock ρ_* and $\rho_* V_*^2$ respectively in the present paper.

It is found that the same coordinate scale introduced in §2 can be used for the solutions both in front of the shock and further downstream of the shock (i.e. outer solution behind the shock), except for a short region, the inner region, immediately behind the shock. The necessary condition of introducing an inner region behind the shock will be discussed in §4.

The asymptotic expansions of the dependent variables for the flows both in front of the shock and further downstream of the shock are assumed to be

$$\left.\begin{aligned}
\mathscr{U}^1 &\sim u_0(\xi)+\delta^2 u_2(\xi,\eta)+\delta^3 u_3(\xi,\eta)+\dots,\\
\mathscr{U}^2 &\sim \quad\delta^2 v_2(\xi,\eta)+\delta^3 v_3(\xi,\eta)+\dots,\\
\rho &\sim r_0(\xi)+\delta^2 r_2(\xi,\eta)+\delta^3 r_3(\xi,\eta)+\dots,\\
p &\sim p_0(\xi)+\delta^2 p_2(\xi,\eta)+\delta^3 p_3(\xi,\eta)+\dots,
\end{aligned}\right\} \tag{17}$$

where the leading terms $O(\delta^0)$ correspond to the one-dimensional solution. As it is easy to show that $\boldsymbol{e}_1$ and $\boldsymbol{e}_2$ in (11) are the vectors parallel to the corresponding coordinates $\eta=$ const and $\xi=$ const, the tangency boundary conditions at the nozzle walls are obviously

$$\mathscr{U}^2=0 \quad \text{on } \eta=\pm 1. \tag{18}$$

Substitution of the assumed form (17) into the differential equations (13)–(16) leads to a sequence of sets of equations for the expansion functions in (17). It is found that only even-order terms of δ are necessary for the solution in front of the shock. For the outer solution behind the shock, however, odd-order terms of δ beginning with terms $O(\delta^3)$ as in (17) are also necessary for the matching with the inner solution behind the shock discussed later.

The zeroth-order governing equations are

$$(fr_0u_0)'=0, \quad r_0u_0u_0'=-p_0', \quad \left(\frac{p_0}{r_0^\gamma}\right)'=0, \tag{19}$$

and their general solutions are

$$\left.\begin{aligned}
u_0\left[\left(C_2+\frac{\gamma-1}{2C_1}\right)-\frac{\gamma-1}{2C_1}u_0^2\right]^{1/(\gamma-1)}&=\frac{1}{f},\\
r_0=\frac{1}{fu_0}, \quad p_0&=\frac{C_1}{\gamma}r_0^\gamma,
\end{aligned}\right\} \tag{20}$$

where C_1 and C_2 are constants yet to be determined.

The governing equations of order δ^2 are found to be

$$[f(r_0u_2+u_0r_2)]_{,\xi}+fr_0v_{2,\eta}=0, \tag{21}$$

$$r_0u_0u_{2,\xi}+u_0'(r_0u_2+u_0r_2)=-p_{2,\xi}+\frac{f'}{f}\eta p_{2,\eta}, \tag{22}$$

$$\frac{f''}{f}\eta r_0 u_0^2 = -\frac{1}{f^2}p_{2,\eta} + \frac{f'}{f}\eta p_0', \tag{23}$$

$$\left(\frac{p_2}{p_0} - \gamma\frac{r_2}{r_0}\right)_{,\xi} = 0. \tag{24}$$

Substituting p_0' of (19) into (23) and integration with respect to η give

$$p_2 = p_{20}(\xi) - \tfrac{1}{2}(u_0 f')'\eta^2, \tag{25}$$

where $p_{20}(\xi)$ is an arbitrary function of ξ yet to be determined. Integration of (24) with respect to ξ gives

$$r_2 = \frac{r_0}{\gamma}\left[\frac{p_2}{p_0} + g_2(\eta)\right], \tag{26}$$

where $g_2(\eta)$is an arbitrary function of η. Then substitution of (25) and (26) into (22) and integration with respect to ξ give

$$u_2 = -\frac{p_{20}}{u_0 r_0} + \frac{g_1(\eta)}{u_0} - \frac{u_0}{2\gamma}g_2(\eta) + \tfrac{1}{2}f^2\left(u_0\frac{f'}{f}\right)'\eta^2, \tag{27}$$

where $g_1(\eta)$ is also an arbitrary function of η. Finally, substitution of (25)–(27) into (21) and integration with respect to η gives

$$v_2 = u_0\left\{\left[\frac{(1-M^2)fp_{20}}{u_0}\right]'\eta - \left(\frac{1}{u_0^2}\right)'\int_0^\eta g_1(\eta)\,\mathrm{d}\eta + \frac{1}{6}\left[f'^2 - (1-M^2)\frac{f}{u_0}(u_0 f')'\right]'\eta^3\right\}, \tag{28}$$

where $M^2 = r_0 u_0^2/\gamma p_0$, and $v_2 = 0$ on $\eta = 0$ has been used to determine the integration constant.

Applying the boundary conditions (18) to (28) yields

$$\left[\frac{(1-M^2)fp_{20}}{u_0}\right]' = \left(\frac{1}{u_0^2}\right)'\int_0^1 g_1(\eta)\,\mathrm{d}\eta - \frac{1}{6}\left[f'^2 - (1-M^2)\frac{f}{u_0}(u_0 f')'\right]',$$

or, after integration,

$$\frac{(1-M^2)fp_{20}}{u_0} = C_3 + \frac{1}{u_0^2}\int_0^1 g_1(\eta)\,\mathrm{d}\eta - \frac{1}{6}\left[f'^2 - (1-M^2)\frac{f}{u_0}(u_0 f')'\right]. \tag{29}$$

This is the equation for evaluating $p_{20}(\xi)$, with C_3 being the integration constant yet to be determined.

Now the expansion functions up to $O(\delta^2)$ in (17) have been obtained in (20) and (25)–(28), with the constants C_1, C_2, C_3 and the functions $g_1(\eta)$, $g_2(\eta)$ yet to be determined. Those constants and functions have to be determined in principle by the upstream conditions.

Obviously, the forms of the solutions are the same for the flows both in front of the shock and further downstream of the shock. To distinguish the solutions for the above two regions, we shall add superscript o to those expansion functions corresponding to the outer solution behind the shock, e.g. $u_0^o, u_2^o, \ldots$.

Let us now determine those constants and functions for the flow field in front of the shock. The flow there is assumed to be potential, so that the entropy and the enthalpy are uniform in the field, i.e.

$$\gamma p/\rho^\gamma = 1, \tag{30}$$

$$\rho^{\gamma-1} = \tfrac{1}{2}(\gamma+1) - \tfrac{1}{2}(\gamma-1)Q^2, \tag{31}$$

where Q is the magnitude of velocity and can be evaluated by

$$Q^2 = g_{ij}\mathscr{U}^i\mathscr{U}^j. \tag{32}$$

It can be shown that, up to order δ^2, (30) is equivalent to

$$\frac{\gamma p_0}{\rho_0^\gamma} = 1, \quad \frac{p_2}{p_0} - \frac{\gamma\rho_2}{\rho_0} = 0, \tag{33a,b}$$

and (31) is equivalent to

$$r_0^{\gamma-1} = \tfrac{1}{2}(\gamma+1) - \tfrac{1}{2}(\gamma-1)\,u_0^2, \tag{34a}$$

$$\frac{r_2}{r_0} = -\frac{u_0 u_2 + \frac{1}{2}f'^2 u_0^2 \eta^2}{\frac{1}{2}(\gamma+1) - \frac{1}{2}(\gamma-1)\,u_0^2}. \tag{34b}$$

Equations (33a) and (34a) show that $C_1 = 1$ and $C_2 = 1$ in (20). It is also easy to show that (33b) and (34b) correspond to $g_2(\eta) = 0$ and $g_1(\eta) = 0$ respectively. Finally, we have $f' = 0$ and $M = 1$ at the throat section. Thus (29) shows that $C_3 = 0$.

So far we have determined all the constants and functions involved in the solution for the flow in front of the shock. For the outer solution behind the shock, those constants and functions are related to the inner solution behind the shock, and will be discussed later. The expansion terms $O(\delta^3)$ in (17) for the outer solution behind the shock are given in Appendix A.

Since $\mathscr{U}^1 = O(1)$, $\mathscr{U}^2 = O(\delta^2)$ by (17) and $|\boldsymbol{e}_1| = O(1)$, $|\boldsymbol{e}_2| = O(\delta)$ by (11), it means that $\eta = \text{const}$ are approximately streamlines of the flow, and the velocity components normal to $\eta = \text{const}$ are only $O(\delta^3)$. *We call this kind of flow the smooth flow in the present paper.* In this case, the transverse pressure gradient is given by (17) and (25) as

$$\frac{\partial p}{\partial \eta} \sim -\delta^2(u_0 f')'\,\eta. \tag{35}$$

Alternatively, we can derive (35) by a more intuitive physical argument. Consider now the y-momentum equation. If $\eta = \text{const}$ are approximately streamlines, we have

$$y\text{-velocity component} \sim u_0\,\delta f'\eta.$$

Thus the y-momentum equation reads

$$\frac{\partial p}{\partial y} \sim -r_0\,u_0(u_0 f')'\,\delta\eta. \tag{36}$$

Keeping in mind that $r_0 u_0 f = 1$ for one-dimensional flow and $y = \delta f\eta$, we again obtain (35).

4. Condition for the disappearance of an inner solution immediately behind the shock

It is well known that, in the case of a weak shock in transonic flow, the flow is singular behind the shock at any point on the wall where the curvature of the wall is continuous and non-zero (see e.g. Ferrari & Tricomi 1968, p. 358), and, for a slender-nozzle flow, an inner solution is needed for the narrow region immediately behind the shock (see e.g. Messiter & Adamson 1975) if $f'' \neq 0$ on the shock position. The extension to the case with a rather strong shock in the present paper will show that the same conclusion holds; except for a particular value of one-dimensional velocity just ahead of the shock, with which an inner solution can disappear even for $f'' \neq 0$.

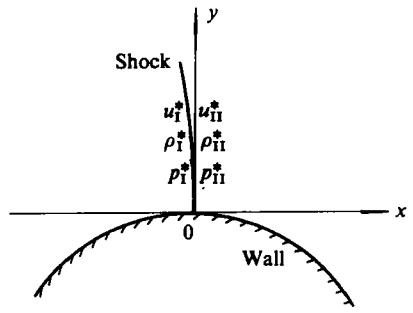

FIGURE 2. Local coordinates at the intersection of the shock and the wall.

Consider a region in the vicinity of the intersection of a shock and wall as shown in figure 2. (x, y) are taken temporarily as the local Cartesian coordinates, with the origin at the intersection point, the x-axis tangential to the wall and pointing downstream, and the y-axis perpendicular to it. The local radius of curvature at the origin is assumed to be $R(\neq \infty$, i.e. $f'' \neq 0)$. According to the shock condition of equality of the tangential velocity components, the shock must be perpendicular to the wall. It is well known that the curvature of the shock, as well as the gradient of the velocity component, is usually logarithmically infinite. However, we can derive a condition at which the singular behaviour of the flow does not exist.

Let u^*, ρ^* and p^* denote the normal velocity component, density and pressure, with subscripts I and II indicating values immediately upstream and downstream of the shock respectively. The difference between the normal velocity component and the magnitude of velocity in the vicinity of the origin is of higher order and can be neglected in the following analysis.

On the one hand, the normal shock conditions require that

$$p_{\mathrm{II}}^* = \frac{\dfrac{\gamma+1}{\gamma-1}u_{\mathrm{I}}^{*2}-1}{\dfrac{\gamma+1}{\gamma-1}-u_{\mathrm{I}}^{*2}}\,p_{\mathrm{I}}^*. \tag{37}$$

The flow in front of the shock is considered to be potential so that u_{I}^* is a function of p_{I}^* satisfying $\mathrm{d}u_{\mathrm{I}}^*/\mathrm{d}p_{\mathrm{I}}^* = -1/\rho_{\mathrm{I}}^* u_{\mathrm{I}}^*$. Then differentiation of (37) with respect to p_{I}^* gives

$$\frac{\mathrm{d}p_{\mathrm{II}}^*}{\mathrm{d}p_{\mathrm{I}}^*} = \frac{u_{\mathrm{I}}^{*2}-\dfrac{\gamma+3}{\gamma+1}}{1-\dfrac{\gamma-1}{\gamma+1}u_{\mathrm{I}}^{*2}}. \tag{38}$$

Equation (38) shows that the sign of $\mathrm{d}p_{\mathrm{II}}^*/\mathrm{d}p_{\mathrm{I}}^*$ required by the shock conditions depends on the value of u_{I}^*. If u_{I}^* is near-transonic, i.e. $u_{\mathrm{I}}^* \sim 1$, then $\mathrm{d}p_{\mathrm{II}}^*/\mathrm{d}p_{\mathrm{I}}^* < 0$, which means that the transverse pressure gradients must have opposite signs immediately on both sides of the shock. If $u_{\mathrm{I}}^* > [(\gamma+3)/(\gamma+1)]^{\frac{1}{2}}$, however, (38) shows that the transverse pressure gradients remain of the same sign on both sides of the shock.

On the other hand, let us consider the y-momentum equation

$$\rho\left(u\frac{\partial v}{\partial x}+v\frac{\partial v}{\partial y}\right) = -\frac{\partial p}{\partial y} \tag{39}$$

at the origin on both sides of the shock, where u and v are the velocity components along the x- and y-directions. In front of the shock we have

$$-\frac{\rho_{\mathrm{I}}^* u_{\mathrm{I}}^{*2}}{R} = -\frac{\partial p_{\mathrm{I}}^*}{\partial y}, \tag{40}$$

as $u = u_{\mathrm{I}}^*$, $\partial v/\partial x = -u_{\mathrm{I}}^*/R$ and $v = 0$. Behind the shock, *if the flow is not singular there*, we similarly have

$$-\frac{\rho_{\mathrm{II}}^* u_{\mathrm{II}}^{*2}}{R} = -\frac{\partial p_{\mathrm{II}}^*}{\partial y}. \tag{41}$$

Combining (40) and (41) yields

$$\frac{\mathrm{d}p_{\mathrm{II}}^*}{\mathrm{d}p_{\mathrm{I}}^*} = \frac{\rho_{\mathrm{II}}^* u_{\mathrm{II}}^{*2}}{\rho_{\mathrm{I}}^* u_{\mathrm{I}}^{*2}} = \frac{u_{\mathrm{II}}^*}{u_{\mathrm{I}}^*} = \frac{1}{u_{\mathrm{I}}^{*2}} \tag{42}$$

along the shock. Obviously, the right-hand sides of (38) and (42) should be the same, and we can thus obtain the condition

$$u_{\mathrm{I}}^{*4} - \frac{4}{\gamma+1} u_{\mathrm{I}}^{*2} - 1 = 0 \tag{43}$$

under which the flow is not singular. For $\gamma = 1.4$ we have

$$u_{\mathrm{I}}^* = u_{\mathrm{I,cr}}^* = \left\{\frac{2}{\gamma+1} + \left[\left(\frac{2}{\gamma+1}\right)^2 + 1\right]^{\frac{1}{2}}\right\}^{\frac{1}{2}} = 1.4612 \tag{44}$$

corresponding to the Mach number $M_{\mathrm{I,cr}}^* = 1.6619$. If the condition (43) is not satisfied, the flow must be singular. In this case, $v_{\mathrm{II}} \to 0$ and $\partial v_{\mathrm{II}}/\partial y \to \infty$ as $y \to 0$ such that the term $v_{\mathrm{II}}\,\partial v_{\mathrm{II}}/\partial y$ has a finite contribution to the y-momentum equation (39), and (41) is then modified such that $\mathrm{d}p_{\mathrm{II}}^*/\mathrm{d}p_{\mathrm{I}}^*$ determined by (40) and (41) should be equal to that determined by (38).

For slender-nozzle flows an analysis based on the asymptotic expansions given in §3 also shows that, when the wall curvature is non-zero, the shock conditions can be fulfilled by the proper choice of the constants C_1, C_2, C_3 in (20), (29) and the functions $g_1(\eta)$, $g_2(\eta)$ in (26), (27) for the outer solution behind the shock without introducing an inner solution immediately behind the shock only if the one-dimensional velocity immediately in front of the shock u_{0*}, instead of u_{I}^*, satisfies (43).

5. Inner solution behind the shock

Section 4 has shown that an inner solution immediately downstream of the shock is necessary, if the wall curvature is non-zero and the one-dimensional velocity just in front of the shock is not equal to the value given by (44).

The shock shape is now assumed to be

$$\xi_{\mathrm{s}} \sim \xi_0 - \delta^2 \tfrac{1}{2} f_0 f_0'(\eta^2 - 1) + \sigma(\delta)\, h(\eta), \tag{45}$$

where subscript s denotes 'shock', ξ_0 is a constant determining the shock position in the nozzle and is obviously dependent on the downstream conditions, and subscript 0 denotes the value of $f(\xi)$ and its derivatives at $\xi = \xi_0$. The first two terms on the right-hand side of (45) in fact represent the one-dimensional shock shape, since it has been shown in §3 that $\eta = \text{const}$ are approximately streamlines for the flow in front of the shock, and (exact to order δ^2) the first two terms on the right-hand side of (45) are the equation of a parabola perpendicular to the streamlines $\eta = \text{const}$

everywhere. It is also temporarily assumed that the correction to the one-dimensional shock shape is of higher order, i.e. $\sigma(\delta) = o(\delta^2)$. It will be proved later in (68) that $\sigma(\delta) = \delta^3$. Then the inner coordinate ξ^i is defined by

$$\xi = \xi_s(\eta) + \delta\xi^i \sim \xi_0 + \delta\xi^i - \delta^2 \tfrac{1}{2} f_0 f_0'(\eta^2 - 1) + \sigma(\delta) h(\eta), \tag{46}$$

with $\xi^i = 0$ corresponding to the shock position.

It is known that the shock conditions require

$$\left.\begin{aligned} V_{t\mathrm{I}} &= V_{t\mathrm{II}} = V_t, \\ V_{n\mathrm{I}} V_{n\mathrm{II}} &= 1 - \frac{\gamma-1}{\gamma+1} V_t^2, \\ \frac{\rho_{\mathrm{II}}}{\rho_{\mathrm{I}}} &= \frac{V_{n\mathrm{I}}}{V_{n\mathrm{II}}}, \\ \frac{p_{\mathrm{II}}}{p_{\mathrm{I}}} &= \left(\frac{\gamma+1}{\gamma-1}\frac{\rho_{\mathrm{II}}}{\rho_{\mathrm{I}}} - 1\right) \Big/ \left(\frac{\gamma+1}{\gamma-1} - \frac{\rho_{\mathrm{II}}}{\rho_{\mathrm{I}}}\right), \end{aligned}\right\} \tag{47}$$

where V_n and V_t are the normal and tangential velocity components respectively. The leading terms of (17) for the outer solution behind the shock (i.e. $\mathscr{U}^1 \sim u_0^0$, $\mathscr{U}^2 \sim 0$, $\rho \sim r_0^0$ and $p \sim p_0^0$) are the one-dimensional solution and are taken as the basis for the inner solution, since it is easy to show that the shock conditions can be satisfied for the leading terms of the solution by proper choice of integration constants in the solution.

It can also be shown from the shock conditions (47) that the correction terms to the one-dimensional solution should be $O(\delta^2)$ for the pressure, density and the velocity component normal to the shock. Let us now analyse the relationship between the normal and tangential velocity components and $\bar{\mathscr{U}}^j$, $\bar{\mathscr{U}}_j$ $(j = 1, 2)$ where (and in what follows) the overbars are used to denote the corresponding quantities for the inner variables. It is known that the velocity vector $\mathscr{U}$ can be expressed as

$$\mathscr{U} = \bar{\mathscr{U}}^j \bar{\boldsymbol{e}}_j = \bar{\mathscr{U}}_j \bar{\boldsymbol{e}}^j, \tag{48}$$

where

$$\bar{\boldsymbol{e}}_k = \frac{\partial x}{\partial X^k}\boldsymbol{i} + \frac{\partial y}{\partial X^k}\boldsymbol{j}, \quad \bar{\boldsymbol{e}}^k = \frac{\partial X^k}{\partial x}\boldsymbol{i} + \frac{\partial X^k}{\partial y}\boldsymbol{j} \quad (k = 1, 2) \tag{49}$$

and

$$X^1 = \xi^i, \; X^2 = \eta.$$

Noting that

$$\bar{\boldsymbol{e}}_2 = \bar{g}_{12}\bar{\boldsymbol{e}}^1 + \bar{g}_{22}\bar{\boldsymbol{e}}^2,$$

we have

$$\mathscr{U} = \frac{\bar{\mathscr{U}}^1}{\bar{g}^{11}}\bar{\boldsymbol{e}}^1 + \frac{\bar{\mathscr{U}}_2}{\bar{g}_{22}}\bar{\boldsymbol{e}}_2. \tag{50}$$

Taking $\xi^i = 0$ in (50) for the shock position, we see that, according to the physical meaning of $\bar{\boldsymbol{e}}^1$ and $\bar{\boldsymbol{e}}_2$, the first term on the right-hand side of (50) is just the normal velocity component, and the second term the tangential velocity component. It can be shown that $|\bar{\boldsymbol{e}}^1| = O(\delta)$ and $\bar{g}^{11} = O(\delta^2)$. Therefore it is concluded from (50) that a correction term $O(\delta^2)$ for the normal velocity component requires a correction term $O(\delta)$ in $\bar{\mathscr{U}}^1$, which accompanies a same-order term in $\bar{\mathscr{U}}^2$ generally required by the governing equations of elliptic type for the inner solution. Thus the asymptotic expansions for the inner solution behind the shock are assumed to be

$$\begin{aligned} \bar{\mathscr{U}}^1 \sim \frac{1}{\delta}\{&u_{0*}^0 + \delta u_{0*}^{0\prime}\xi^i + \delta^2[\tfrac{1}{2}u_{0*}^{0\prime\prime}\xi^{i2} - \tfrac{1}{2}u_{0*}^{0\prime} f_0 f_0'(\eta^2 - 1) + U_2(\xi^i, \eta)] \\ &+ \delta^3[\tfrac{1}{6}u_{0*}^{0\prime\prime\prime}\xi^{i3} - \tfrac{1}{2}u_{0*}^{0\prime\prime} f_0 f_0'\xi^i(\eta^2 - 1) + U_3(\xi^i, \eta)] + \sigma(\delta)u_{0*}^{0\prime} h\}, \end{aligned} \tag{51a}$$

$$\overline{\mathscr{U}}^2 \sim \delta V_2(\xi^1,\eta)+\delta^2 V_3(\xi^1,\eta), \tag{51b}$$

$$\rho \sim r^0_{0*}+\delta r^{0\prime}_{0*}\xi^1+\delta^2[\tfrac{1}{2}r^{0\prime\prime}_{0*}\xi^{12}-\tfrac{1}{2}r^{0\prime}_{0*}f_0 f_0'(\eta^2-1)+R_2(\xi^1,\eta)] + \delta^3[\tfrac{1}{6}r^{0\prime\prime\prime}_{0*}\xi^{13}-\tfrac{1}{2}r^{0\prime\prime}_{0*}f_0 f_0'\xi^1(\eta^2-1)+R_3(\xi^1,\eta)]+\sigma(\delta)\,r^{0\prime}_{0*}h, \tag{51c}$$

$$p \sim p^0_{0*}+\delta p^{0\prime}_{0*}\xi^1+\delta^2[\tfrac{1}{2}p^{0\prime\prime}_{0*}\xi^{12}-\tfrac{1}{2}p^{0\prime}_{0*}f_0 f_0'(\eta^2-1)+P_2(\xi^1,\eta)] + \delta^3[\tfrac{1}{6}p^{0\prime\prime\prime}_{0*}\xi^{13}-\tfrac{1}{2}p^{0\prime\prime}_{0*}f_0 f_0'\xi^1(\eta^2-1)+P_3(\xi^1,\eta)]+\sigma(\delta)\,p^{0\prime}_{0*}h, \tag{51d}$$

where $U_j(\xi^1,\eta)$, $V_j(\xi^1,\eta)$, $R_j(\xi^1,\eta)$, $P_j(\xi^1,\eta)$ $(j=2,3)$ are the expansion functions to be determined for the inner solution, and subscript $*$ denotes values at $\xi=\xi_0$.

The governing equations for the correction terms $O(\delta^2)$ are found to be

$$\left.\begin{aligned} U_{2,\xi^1}+V_{2,\eta}+f_0\,u^{02}_{0*}R_{2,\xi^1} &= 0,\\ r^0_{0*}u^0_{0*}U_{2,\xi^1}+P_{2,\xi^1} &= 0,\\ f_0\,V_{2,\xi^1}+P_{2,\eta} &= -(u^0_0 f')'_*\eta,\\ u^{02}_{0*}R_{2,\xi^1}-M_0^2\,P_{2,\xi^1} &= 0, \end{aligned}\right\} \tag{52}$$

where $M_0^2 = r^0_{0*}u^{02}_{0*}/\gamma p^0_{0*}$. Equations (52) can be derived from a set of equations similar to (13)–(16) with streamwise coordinate ξ^1 instead of ξ. This is a non-homogeneous set of equations for U_2, V_2, R_2 and P_2, and the boundary conditions on the walls are

$$V_2(\xi^1,\pm 1)=0. \tag{53}$$

The non-homogeneous part of the solution for (52) is simply $U_2=V_2=R_2=0$, $P_2=-\frac{1}{2}(u^0_0 f')'_*\eta^2$, and the general solution for the homogeneous part can be obtained by the method of separation of variables. Therefore the general solution for (52) can be written as

$$\left.\begin{aligned} U_2 &= u^0_{0*}\left\{F_1(\eta)-\frac{1}{\gamma M_0^2}H\left(\frac{\xi^1}{\beta_0 f_0},\eta\right)\right\},\\ V_2 &= -\frac{\beta_0 u^0_{0*}}{M_0^2 f_0}K\left(\frac{\xi^1}{\beta_0 f_0},\eta\right),\\ R_2 &= r^0_{0*}\left\{F_2(\eta)+\frac{1}{\gamma}H\left(\frac{\xi^1}{\beta_0 f_0},\eta\right)\right\},\\ P_2 &= -\tfrac{1}{2}(u^0_0 f')'_*\eta^2+p^0_{0*}H\left(\frac{\xi^1}{\beta_0 f_0},\eta\right), \end{aligned}\right\} \tag{54}$$

where

$$\left.\begin{aligned} H(\zeta,\eta) &= \sum_{n=0}^{\infty} e_n\,\mathrm{e}^{-n\pi\zeta}\cos n\pi\eta,\\ K(\zeta,\eta) &= \sum_{n=1}^{\infty} e_n\,\mathrm{e}^{-n\pi\zeta}\sin n\pi\eta. \end{aligned}\right\} \tag{55}$$

$F_1(\eta)$ and $F_2(\eta)$ in (54) are arbitrary functions to be determined by the shock conditions, so are the arbitrary constants e_n $(n=0,1,2,\ldots)$ in (55). Now we can use the shock conditions (47) to determine those functions and constants, and also the constants C_1 and C_2 in (20). The solution in front of the shock has been given in §2. Substituting $\xi=\xi_s$ given by (45) into the solution, we can obtain the velocity components, density and pressure immediately before the shock. Note that the

normal velocity component corresponding to the first term on the right-hand side of (50). In this way, we obtain

$$\left.\begin{aligned} &V_{t\mathrm{I}} = O(\delta^2),\\ &V_{n\mathrm{I}} \sim u_{0*}\left\{1+\delta^2\left[\left(\frac{u_{20*}}{u_{0*}}+\tfrac{1}{2}f_0f_0'\frac{u_{0*}'}{u_{0*}}\right)+\tfrac{1}{2}f_0f_0''\eta^2\right]\right\},\\ &\rho_{\mathrm{I}} \sim r_{0*}\left\{1+\delta^2\left[\left(\frac{r_{20*}}{r_{0*}}+\tfrac{1}{2}f_0f_0'\frac{r_{0*}'}{r_{0*}}\right)+\left(\frac{r_{22*}}{r_{0*}}-\tfrac{1}{2}f_0f_0'\frac{r_{0*}'}{r_{0*}}\right)\eta^2\right]\right\},\\ &p_{\mathrm{I}} \sim p_{0*}\left\{1+\delta^2\left[\left(\frac{p_{20*}}{p_{0*}}+\tfrac{1}{2}f_0f_0'\frac{p_{0*}'}{p_{0*}}\right)+\left(\frac{p_{22*}}{p_{0*}}-\tfrac{1}{2}f_0f_0'\frac{p_{0*}'}{p_{0*}}\right)\eta^2\right]\right\}. \end{aligned}\right\} \tag{56}$$

A similar procedure can be applied for the variables immediately behind the shock to obtain

$$\left.\begin{aligned} &V_{n\mathrm{II}} \sim u_{0*}^0\left\{1+\delta^2\left[\tfrac{1}{2}f_0f_0'\frac{u_{0*}^{0\prime}}{u_{0*}^0}(1-\eta^2)+\tfrac{1}{2}f_0'^2\eta^2+F_1(\eta)-\frac{1}{\gamma M_0^2}H(0,\eta)\right]\right\},\\ &\rho_{\mathrm{II}} \sim r_{0*}^0\left\{1+\delta^2\left[\tfrac{1}{2}f_0f_0'\frac{r_{0*}^{0\prime}}{r_{0*}^0}(1-\eta^2)+F_2(\eta)+\frac{1}{\gamma}H(0,\eta)\right]\right\},\\ &p_{\mathrm{II}} \sim p_{0*}^0\left\{1+\delta^2\left[\tfrac{1}{2}f_0f_0'\frac{p_{0*}^{0\prime}}{p_{0*}^0}(1-\eta^2)-\tfrac{1}{2}(u_0^0f')_*'\eta^2+H(0,\eta)\right]\right\}. \end{aligned}\right\} \tag{57}$$

The factors before the curly brackets in (56) and (57) are obviously the one-dimensional velocities, densities and pressures immediately upstream and downstream of the shock. It is easy to show that the shock conditions (47) for the leading terms in (56) and (57) can be satisfied by choosing

$$\left.\begin{aligned} &C_1 = \left(\frac{\gamma+1}{\gamma-1}u_{0*}^2-1\right)\Big/\left[u_{0*}^{2\gamma}\left(\frac{\gamma+1}{\gamma-1}-u_{0*}^2\right)\right],\\ &C_2 = (r_{0*}u_{0*}^2)^{\gamma-1}-\frac{\gamma-1}{2C_1}\left(1-\frac{1}{u_{0*}^2}\right) \end{aligned}\right\} \tag{58}$$

for u_{0*}^0, r_{0*}^0 and p_{0*}^0 in (20). For the $O(\delta^2)$ terms in (56) and (57), the shock conditions (47) also show that $H(0,\eta)$ must be of the form

$$H(0,\eta) = \sum_{n=0}^{\infty} e_n \cos n\pi\eta = \alpha_3+\beta_3\eta^2, \tag{59}$$

with constants α_3 and β_3 satisfying

$$\left.\begin{aligned} &\alpha_3+\tfrac{1}{2}f_0f_0'\frac{p_{0*}^{0\prime}}{p_{0*}^0} = \frac{p_{20*}}{p_{0*}}+\tfrac{1}{2}f_0f_0'\frac{p_{0*}'}{p_{0*}}+k_p\left(\frac{u_{20*}}{u_{0*}}+\tfrac{1}{2}f_0f_0'\frac{u_{0*}'}{u_{0*}}\right),\\ &\beta_3-\tfrac{1}{2}f_0f_0'\frac{p_{0*}^{0\prime}}{p_{0*}^0}-\frac{(u_0^0f')_*'}{2p_{0*}^0} = \frac{p_{22*}}{p_{0*}}-\tfrac{1}{2}f_0f_0'\frac{p_{0*}'}{p_{0*}}+\tfrac{1}{2}k_pf_0f_0'', \end{aligned}\right\} \tag{60}$$

where

$$k_p = \frac{8\gamma}{(\gamma+1)^2}u_{0*}^2\Big/\left[\left(u_{0*}^2-\frac{\gamma-1}{\gamma+1}\right)\left(1-\frac{\gamma-1}{\gamma+1}u_{0*}^2\right)\right]. \tag{61}$$

Similarly, $F_1(\eta)$ and $F_2(\eta)$ must be of the form

$$F_j(\eta) = \alpha_j+\beta_j\eta^2 \quad (j=1,2), \tag{62}$$

with constants α_j, β_j $(j = 1, 2)$ satisfying

$$\left.\begin{aligned} \alpha_1 - \frac{\alpha_3}{\gamma M_0^2} + \tfrac{1}{2} f_0 f_0' \frac{u_{0*}^{0\prime}}{u_{0*}^0} &= -\left(\frac{u_{20*}}{u_{0*}} + \tfrac{1}{2} f_0 f_0' \frac{u_{0*}'}{u_{0*}}\right), \\ \beta_1 - \frac{\beta_3}{M_0^2} - \tfrac{1}{2} f_0 f_0' \frac{u_{0*}^{0\prime}}{u_{0*}^0} &= -\tfrac{1}{2}(f_0 f_0'' + f_0'^2), \end{aligned}\right\} \tag{63}$$

$$\left.\begin{aligned} \alpha_2 + \frac{\alpha_3}{\gamma} + \tfrac{1}{2} f_0 f_0' \frac{r_{0*}^{0\prime}}{r_{0*}^0} &= \frac{r_{20*}}{r_{0*}} + \tfrac{1}{2} f_0 f_0' \frac{r_{0*}'}{r_{0*}} + \frac{1}{2}\left(\frac{u_{20*}}{u_{0*}} + f_0 f_0' \frac{u_{0*}'}{u_{0*}}\right), \\ \beta_2 + \frac{\beta_3}{\gamma} - \tfrac{1}{2} f_0 f_0' \frac{r_{0*}^{0\prime}}{r_{0*}^0} &= \frac{r_{22*}}{r_{0*}} - \tfrac{1}{2} f_0 f_0' \frac{r_{0*}'}{r_{0*}} + f_0 f_0''. \end{aligned}\right\} \tag{64}$$

Equations (60), (63) and (64) are used to determine the constants α_j, β_j $(j = 1, 2, 3)$. Specifically, if the one-dimensional flow relations and shock conditions are used for the second relation of (60), it can be shown that

$$\beta_3 = \frac{\dfrac{\gamma}{\gamma+1}\left(1 + \dfrac{4}{\gamma+1} u_{0*}^2 - u_{0*}^4\right)}{\left(u_{0*}^2 - \dfrac{\gamma-1}{\gamma+1}\right)\left(1 - \dfrac{\gamma-1}{\gamma+1} u_{0*}^2\right)} f_0 f_0''. \tag{65}$$

Note that only the terms of e_n $(n \neq 0)$ in (55) contain the inner coordinate ξ^1 in the solution of (54), and represent the relatively rapid varying of the variables in the streamwise direction. If $\beta_3 = 0$, we have $e_0 = \alpha_3$ and $e_n = 0$ for $n \neq 0$ from (59). In this case it can be shown that the inner expansions of (51 *a–d*) are identically the inner limits of the outer expansions. In other words, the inner solution disappears. It is expected that $\beta_3 = 0$ is equivalent to condition (43), with u_1^* replaced by u_{0*} for slender-nozzle flows.

Finally, the function $\sigma(\delta)\,\mathrm{h}(\eta)$ is determined by the equality of the tangential velocity components on both sides of the shock. According to (50), this condition is equivalent to the equality of $\overline{\mathscr{U}}_2$ immediately upstream and downstream of the shock. Using the transformation

$$\overline{\mathscr{U}}_2 = \bar{g}_{12}\,\overline{\mathscr{U}}^1 + \bar{g}_{22}\,\overline{\mathscr{U}}^2, \tag{66}$$

it is found that

$$\left.\begin{aligned} \overline{\mathscr{U}}_{2,\,\mathrm{I}} &\sim \delta^3 u_{0*} h', \\ \overline{\mathscr{U}}_{2,\,\mathrm{II}} &\sim \sigma(\delta)\, u_{0*}^0 h' + \delta^3 f_0^2\, V_2(0, \eta). \end{aligned}\right\} \tag{67}$$

Thus the shock condition requires

$$\sigma(\delta) = \delta^3 \tag{68}$$

and

$$(u_{0*} - u_{0*}^0)\, h'(\eta) = f_0^2\, V_2(0, \eta). \tag{69}$$

Equation (69) is the ordinary differential equation for $h(\eta)$. Note that the solution for e_n from (59) is

$$\left.\begin{aligned} e_0 &= \alpha_3 + \tfrac{1}{3}\beta_3, \\ e_n &= \frac{4(-1)^n}{\pi^2 n^2}\beta_3 \quad (n = 1, 2, 3, \ldots), \end{aligned}\right\} \tag{70}$$

and

$$K(\zeta, \eta) = \frac{4\beta_3}{\pi^2} \sum_{n=1}^{\infty} \frac{(-1)^n}{n^2} \mathrm{e}^{-n\pi\zeta} \sin n\pi\eta. \tag{71}$$

Substitution of (71) into (54) and letting $\xi^i = 0$ yield

$$V_2(0,\eta) = -\frac{4\beta_0\beta_3 u_{0*}^0}{\pi^2\gamma M_0^2 f_0}\sum_{n=1}^{\infty}\frac{(-1)^n}{n^2}\sin n\pi\eta. \tag{72}$$

Then, on substitution of (72) into (69) and integration with respect to η, we have

$$h(\eta) = \frac{4\beta_0\beta_3 u_{0*}^0 f_0}{\pi^3\gamma M_0^2(u_{0*}-u_{0*}^0)}\sum_{n=1}^{\infty}\frac{(-1)^n}{n^3}[\cos n\pi\eta-(-1)^n], \tag{73}$$

where $h(1) = 0$ is chosen to determine the constant of integration, which means $\xi = \xi_0$ is assumed to be the shock position on the wall (see (45)).

It is also important to include one more term in each of U_3, V_3, R_3, P_3 in (51*a–d*) to improve the accuracy of the solution, and one more term is also added to (45) as

$$\xi_s \sim \xi_0 - \delta^2\tfrac{1}{2}f_0 f_0'(\eta^2-1)+\delta^3 h(\eta)+\delta^4 k(\eta). \tag{74}$$

The deduction is simple in principle, but the process is tedious. Only the results are given in Appendix B for brevity.

6. Matching procedure and the composite solution

So far the constant C_3 and the functions $g_1(\eta)$ and $g_2(\eta)$ introduced in the outer solution have yet to be determined, and we can do this by considering the matching between the inner and the outer solutions behind the shock.

First consider the matching of the pressure fields. As the outer expansion of the inner solution, the terms in $H(\zeta,\eta)$ of (55) are all the transcendentally small terms, except for the leading term e_0. Therefore the outer expansion of the inner solution for pressure p can be written as

$$p \sim p_{0*}^0+\delta p_{0*}^{0\prime}\xi^i+\delta^2[\tfrac{1}{2}p_{0*}^{0\prime\prime}\xi^{i2}-\tfrac{1}{2}p_{0*}^{0\prime}f_0 f_0'(\eta^2-1)-\tfrac{1}{2}(u_0^0 f')_*'\eta^2+p_{0*}^0 e_0]. \tag{75}$$

On the other hand, the inner expansion of the outer solution for pressure can be derived from (17), (25) and (29) as

$$p \sim p_{0*}^0+\delta p_{0*}^{0\prime}\xi^i+\delta^2[\tfrac{1}{2}p_{0*}^{0\prime\prime}\xi^{i2}-\tfrac{1}{2}p_{0*}^{0\prime}f_0 f_0'(\eta^2-1)+p_{20*}^0-\tfrac{1}{2}(u_0^0 f')_*'\eta^2], \tag{76}$$

where

$$p_{20*}^0 = \frac{u_{0*}^0}{(1-M_0^2)f_0}\left\{C_3+\frac{1}{u_{0*}^{02}}\int_0^1 g_1(\eta)\,d\eta-\tfrac{1}{3}[f_0'^2-\tfrac{1}{2}(1-M_0^2)f_0 f_0'']\right\}. \tag{77}$$

Then the Van Dyke matching principle requires that

$$p_{20*}^0 = p_{0*}^0 e_0. \tag{78}$$

Similarly, the matching of the density fields requires that

$$g_2(\eta) = a_2+b_2\eta^2, \tag{79}$$

with constants a_2 and b_2 satisfying

$$\alpha_2 = \frac{a_2}{\gamma}, \quad \beta_2 = \frac{b_2}{\gamma}+\frac{p_{22*}^0}{p_{0*}^0\gamma}, \tag{80}$$

and the matching of velocity fields requires that

$$g_1(\eta) = a_1+b_1\eta^2 \tag{81}$$

with constants a_1 and b_1 satisfying

$$\left.\begin{aligned} u^0_{0*}\alpha_1 &= \frac{a_1}{u^0_{0*}} - \frac{u^0_{0*}}{2}a_2, \\ u^0_{0*}\beta_1 &= \frac{b_1}{u^0_{0*}} - \frac{u^0_{0*}}{2\gamma}b_2 + \tfrac{1}{2}f_0^2\left(u_0^0\frac{f'}{f}\right)'_*. \end{aligned}\right\} \tag{82}$$

Thus we can evaluate a_2 and b_2 from (80), then a_1 and b_1 from (82), and finally C_3 from (77) and (78).

The additive rule is used to construct the composite solution. If the superscript c is used to denote composite solutions, we have

$$\mathscr{U}^{1c} \sim u_0^0 + \delta^2\left[u_2^0 - \frac{4\beta_3 u^0_{0*}}{\pi^2\gamma M_0^2}\sum_{n=1}^{\infty}\frac{(-1)^n}{n^2}\,\mathrm{e}^{-n\pi\xi^1/\beta_0 f_0}\cos n\pi\eta\right], \tag{83a}$$

$$\mathscr{U}^{2c} \sim \delta^2 v_2^0, \tag{83b}$$

$$\rho^c \sim r_0^0 + \delta^2\left[r_2^0 + \frac{4\beta_3 r^0_{0*}}{\pi^2\gamma}\sum_{n=1}^{\infty}\frac{(-1)^n}{n^2}\,\mathrm{e}^{-n\pi\xi^1/\beta_0 f_0}\cos n\pi\eta\right], \tag{83c}$$

$$p^c \sim p_0^0 + \delta^2\left[p_2^0 + \frac{4\beta_3 p^0_{0*}}{\pi^2}\sum_{n=1}^{\infty}\frac{(-1)^n}{n^2}\,\mathrm{e}^{-n\pi\xi^1/\beta_0 f_0}\cos n\pi\eta\right]. \tag{83d}$$

7. Illustrative examples and discussion

Figure 3(*a*) shows the shapes of the shock for five different streamwise shock locations in a hyperbolic nozzle of $f(x) = (1+x^2)^{\frac{1}{2}}$ and $\delta = (0.1)^{\frac{1}{2}}$ in (1). In this case the radius of curvature at the throat $R_0 = \delta^{-1}$, the half-throat height $H_0 = \delta$ and the ratio of the two $R_0/H_0 = \delta^{-2} = 10$. In the present theory the truncation error is $O(\delta^4)$, and hence $O(0.01)$ in the example. The middle case is for $\xi_0 = 0.83495$, corresponding to the case without inner solution. Note that in figure 3(*a*) the half-throat height H_0 is taken as the unit of length. The shape is evaluated from (74). The second term on the right-hand side of (74) is a parabola perpendicular to the nozzle wall. This means that the dominant term for the shock shape corresponds to a curve convex to the downstream direction for the hyperbolic nozzle. However, figure 3(*a*) shows that, for the shock position near the throat, the shock shape shows a reversal of curvature in the transverse direction (as earlier pointed out in Messiter & Adamson (1975) and shown graphically in Lin & Shen (1982)). A more physical explanation is as follows. For a transonic shock with $\xi_0 = O(\delta)$, we have $f_0' = O(\delta)$ and

$$-\delta^2\tfrac{1}{2}f_0 f_0'(\eta^2-1) = O(\delta^3), \tag{84}$$

Also, it can be shown that $u_{0*} - u^0_{0*} = O(\delta)$ and $\beta_0^2 = O(\delta)$ for transonic shock. Thus from (73) we have $h(\eta) = O(\delta^{-\frac{1}{2}})$ and

$$\delta^3 h(\eta) = O(\delta^{\frac{5}{2}}), \tag{85}$$

which plays a more important part in (74) than the term given by (84). Noting that the half-width at the throat is $H_0 = \delta f(0) = \delta$, it turns out that $\delta^3 h(\eta)/H_0 = O(\delta^{\frac{3}{2}})$, which is of the same order as the term $x'(y; E)$ given by equation (53) of Messiter & Adamson (1975), or the term $\tau^3 g_1^p(\eta)$ given by equation (33) of Lin & Shen (1982). In fact it can be shown for the transonic limit that

$$\frac{\delta^3 h(\eta)}{H_0} \sim -\delta^{\frac{3}{2}}\frac{2(\gamma+1)^{\frac{3}{4}}}{\pi^2 x_0^{\frac{1}{2}}}\sum_{n=1}^{\infty}\frac{(-1)^n}{n^2}\sin n\pi\eta,$$

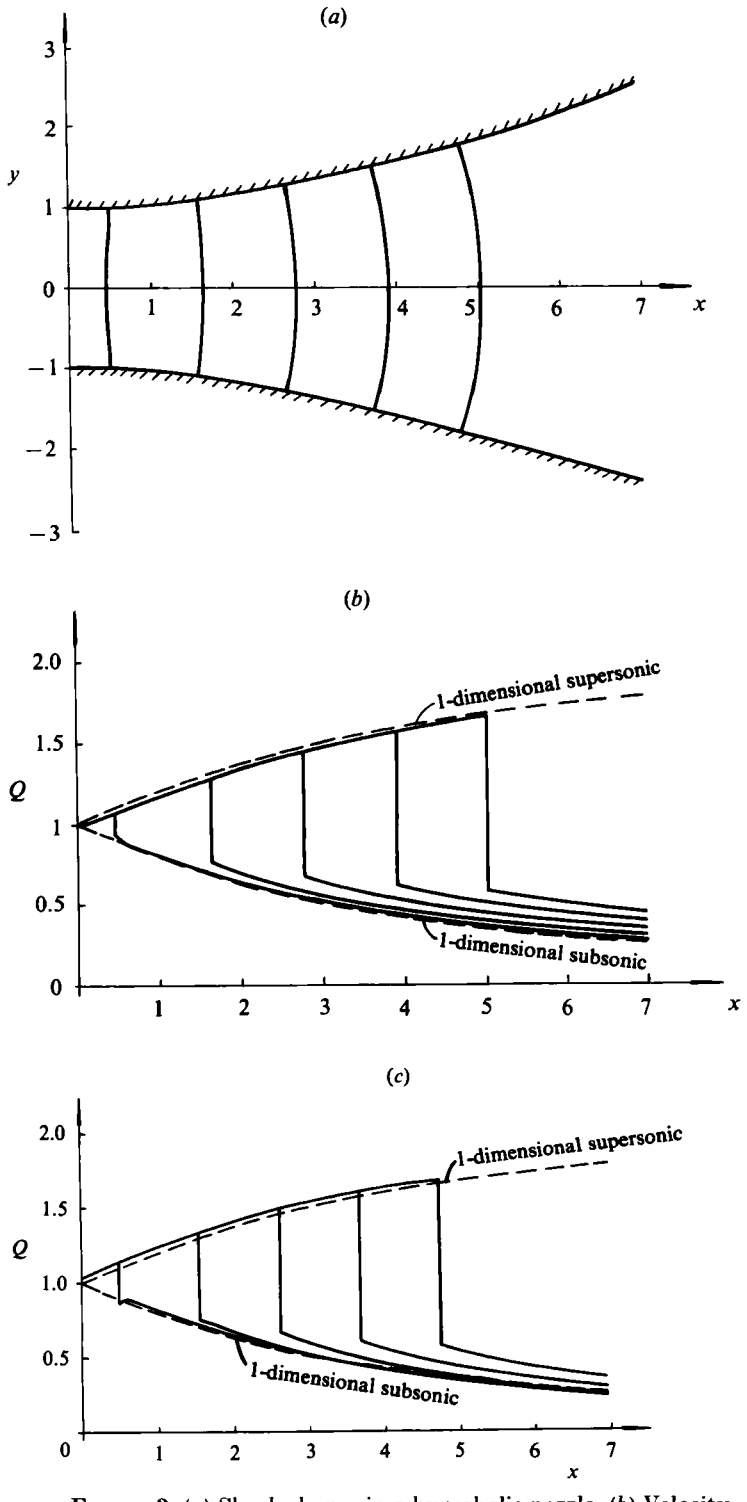

FIGURE 3. (a) Shock shapes in a hyperbolic nozzle. (b) Velocity distribution on axis. (c) Velocity distribution on wall.

if we take $\xi_0 = \delta x_0$. It is easy to show that the above expression is quantitatively the same as $x'(y; E)$ given by Messiter & Adamson (1975).

Obviously, the shock location in the nozzle is determined by the upstream and downstream conditions of the flow. The appropriate shock location produces an entropy jump across the shock and corresponding flow parameters which are compatible with those conditions. As the normal velocity component $V_{n\mathrm{I}}$ immediately in front of the shock can be estimated as

$$V_{n\mathrm{I}} \sim |\mathscr{U}^1 e_1|_{\xi=\xi_S} \sim u_{0*} + \delta^2 \left[\left(\frac{-p_{20*}}{u_{0*} r_{0*}} + \tfrac{1}{2} f_0 f_0' u_{0*}' \right) + \tfrac{1}{2} f_0 f_0'' u_{0*} \eta^2 \right] \tag{86}$$

and the tangential velocity component V_t can be estimated as $O(\delta^3)$, the entropy jump across the shock can be evaluated as

$$\begin{aligned} \frac{s_{\mathrm{II}} - s_{\mathrm{I}}}{R} &= \frac{1}{\gamma - 1} \log \left[\left(\frac{p_{\mathrm{II}}}{p_{\mathrm{I}}} \right) \Big/ \left(\frac{\rho_{\mathrm{II}}}{\rho_{\mathrm{I}}} \right)^{\gamma} \right] \\ &= \frac{1}{\gamma - 1} \log \left\{ \left(\frac{\gamma+1}{\gamma-1} V_{n\mathrm{I}}^2 - 1 \right) \Big/ \left[V_{n\mathrm{I}}^{2\gamma} \left(\frac{\gamma+1}{\gamma-1} - V_{n\mathrm{I}}^2 \right) \right] \right\} + o(\delta^2), \end{aligned} \tag{87}$$

where s is the entropy and R is the gas constant. The asymptotic expansion of (87) can be obtained by substitution of (86) into (87). If the shock strength is not weak, i.e. $\xi_0 = O(1)$ and $u_{0*} - 1 = O(1)$, we can estimate that the leading term of (87) is $O(1)$ and is constant along the shock, and the second term is $O(\delta^2)$ and is variable along the shock. Therefore the present theory evaluates the vorticity of order δ^2 behind the shock. However, if the shock strength is weak, i.e. $\xi_0 = O(\delta)$ and $u_{0*} - 1 = O(\delta)$, the present theory agrees with that of Messiter & Adamson (1975) or Lin & Shen (1982), with the entropy jump across the shock being $O(\delta^3)$ and the vorticity behind the shock $O(\delta^4)$.

Figures 3 (*b*, *c*) show the velocity distributions on the nozzle axis and the wall given by (83*a*) due to the different shock positions. The isentropic one-dimensional velocities for both subsonic and supersonic flows are also given by the dotted lines. The different velocity distributions behind the shock due to the different entropy jumps are clearly seen. Also, for the case with the leftmost shock position, the influence of the inner solution on the velocity distribution can be seen. In this case $u_{0*} < u_{0*,\mathrm{cr}}$ and the velocity immediately behind the shock is higher near the axis, and lower on the wall, than that required by the smooth-flow solution. The inner solution thus provides locally the necessary adjustment. However, as shown from the figures, this effect of the inner solution becomes less prominent as the shock position moves downstream. To understand this feature, we recall that the thickness of inner solution is of order $\beta_0 \delta$, because the rapid change of the flow parameters of the inner solution is manifested by the factor $\pi \xi^1 / \beta_0 f_0$ in the exponential functions in (83*a–d*). As the shock position moves towards the throat, the shock strength is weaker, β_0 is smaller, and the inner solution provides a steeper velocity gradient, and hence stronger influence on the velocity distribution. In contrast, as the shock position moves downstream, the inner region becomes thicker because β_0 increases to order 1, and the influence of the inner solution becomes less noticeable. Incidentally, in the present example, the value of δ is $(0.1)^{\frac{1}{2}} = 0.3162$, which is not too small compared with 1, and the velocity distributions due to the outer solution essentially prevail.

Figure 4 illustrates qualitatively the phenomenon of inviscid shock-induced separation. The nozzle wall is described by

$$h = \delta(3.2 - 1.5\, \mathrm{e}^{-x^2}),$$

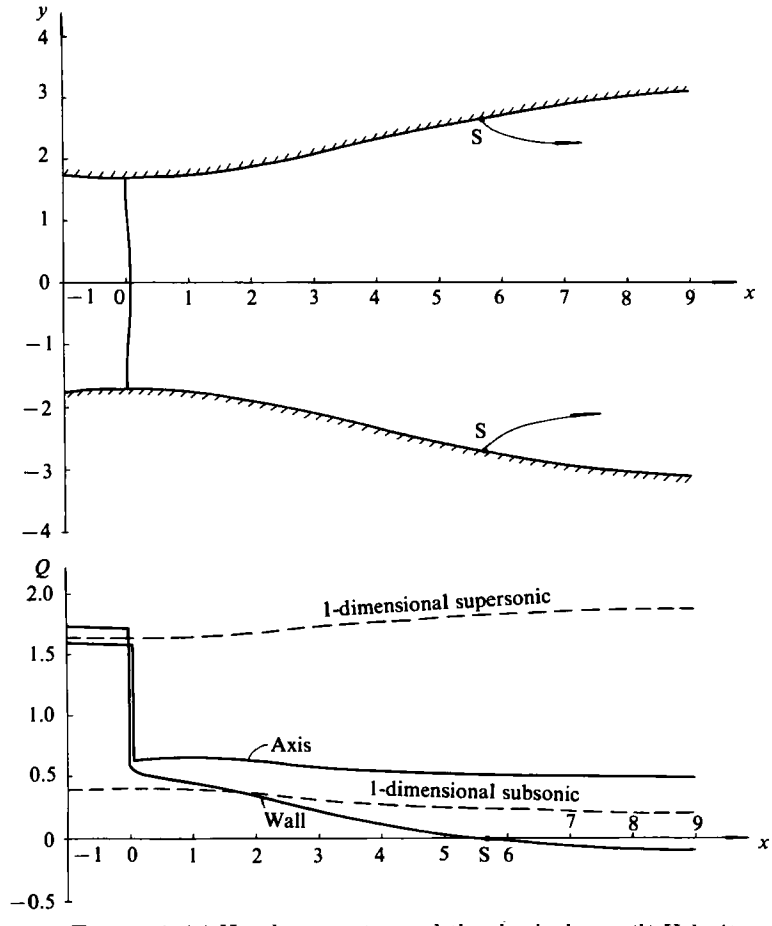

FIGURE 4. (*a*) Nozzle geometry and the shock shape. (*b*) Velocity distribution along the axis and the wall.

with $\delta = 0.18257$. The one-dimensional velocity at the throat is assumed to be supersonic, and a shock is formed near the throat with $\xi_0 = 0$. The streamline along the wall has the strongest shock strength and the largest entropy jump. As the flow behind the shock is decelerated downstream, the flow near the wall loses all its kinetic energy at some separation point S, whereas the rest of the flow still goes forward. The truncated error is of order 0.001 for this example. The one-dimensional velocity distributions for both subsonic and supersonic flows are also shown by the dotted lines in figure 4 for comparison.

While illuminating, the result may not be quantitatively correct, at least for the following two reasons. First, the velocity approaches zero at the vicinity of the separation point, and the governing equations become singular there. For instance, we can see from (27) that, as u_0^0 approaches zero, the first two terms on the right-hand side are no longer of order 1. Secondly, the smooth-flow assumption is obviously not valid with separation. As in viscous boundary layers, the separation region cannot be analysed without further information concerning the total energy and entropy of the reverse flow inside that region. Further analysis of this phenomenon has not been attempted.

8. Conclusion

Previous research applying the asymptotic-expansion method to transonic flows with shock in slender nozzles is extended to handle a wider speed range from low subsonic to supersonic flows with proper account of the vorticity behind the shock. The small parameter describing the slenderness of the nozzle in (1) is used as an expansion quantity. For the flow in front of the shock, as well as the flow further downstream of the shock, a coordinate scale is chosen such that the governing equations are reduced to the parabolic type, irrespective of its original type, which is elliptic or hyperbolic depending on the flow speed. The solution for the flow in front of the shock is expanded in ascending even powers of δ, whereas the solution for the flow further downstream of the shock also contains terms of odd powers of δ beginning with $O(\delta^3)$ and required by the matching with the inner solution immediately behind the shock. According to such an expansion, the flow exact to the order of δ^2 is so smooth that the streamlines are all affinely similar to the nozzle wall, and the transverse pressure gradient is determined by the local nozzle shape given by (35).

For the flow immediately behind the shock, however, the transverse pressure gradient is determined by the shock conditions rather than the local nozzle shape, and an inner solution is generally necessary there to act as a transition region for the pressure distributions to change from one type to the other. The coordinate scaling for the inner region is so chosen that the governing equations retain their original elliptic type. The well-known singularity of the flow just behind the shock point at the wall is related to the inner solution. Meanwhile, a critical shock location at which the inner solution disappears is found, and the transverse pressure gradient required by the local nozzle shape is coincident with that required by the shock conditions in this case.

A numerical example qualitatively shows evidence of the phenomenon of inviscid shock-induced separation: the flow may separate from the wall owing to the combination of larger entropy jump across the shock and sustained deceleration. Like a viscous boundary layer, the loss of mechanical energy near the wall is the key mechanism, except that entropy instead of friction is responsible.

Appendix A. Terms $O(\delta^3)$ in (17) for the outer solution behind the shock

Governing equations of order δ^3 can be derived as

$$[f(r_0^0 u_3^0 + u_0^0 r_3^0)]_{,\xi} + f r_0^0 v_{3,\eta}^0 = 0, \tag{A 1}$$

$$r_0^0 u_0^0 u_{3,\xi}^0 + u_0^{0\prime}(r_0^0 u_3^0 + u_0^0 r_3^0) = -p_{3,\xi}^0 + \frac{f'}{f}\eta p_{3,\eta}^0, \tag{A 2}$$

$$p_{3,\eta}^0 = 0, \tag{A 3}$$

$$\left(\frac{p_3^0}{p_0^0} - \gamma\frac{r_3^0}{r_0^0}\right)_{,\xi} = 0. \tag{A 4}$$

Equations (A 3), (A 4), (A 2) and (A 1) can be solved in turn to obtain

$$p_3^0 = f_3(\xi), \tag{A 5}$$

$$r_3^0 = \frac{r_0^0}{\gamma}\left\{\frac{f_3(\xi)}{p_0^0} + g_4(\eta)\right\}, \tag{A 6}$$

$$u_3^0 = -\frac{u_0^0}{2\gamma} g_4(\eta) + \frac{1}{u_0^0} g_3(\eta) - f f_3(\xi), \tag{A 7}$$

$$v_3^0 = u_0^0 \left\{ \left[\frac{f(1-M^2)}{u_0^0} f_3(\xi) \right]' \eta - \left(\frac{1}{u_0^{02}} \right)' \int_0^\eta g_3(\eta)\, \mathrm{d}\eta \right\}, \tag{A 8}$$

where $f_3(\xi)$, $g_3(\eta)$ and $g_4(\eta)$ are arbitrary functions introduced after integration and yet to be determined.

Applying the boundary condition (18) to (A 8) yields

$$\left[\frac{f(1-M^2)}{u_0^0} f_3(\xi) \right]' - \left(\frac{1}{u_0^{02}} \right)' \int_0^1 g_3(\eta)\, \mathrm{d}\eta = 0,$$

or, after integration with respect to ξ,

$$\frac{f(1-M^2)}{u_0^0} f_3(\xi) = C_4 + \frac{1}{u_0^{02}} \int_0^1 g_3(\eta)\, \mathrm{d}\eta. \tag{A 9}$$

Then the integration constant C_4 and the functions $g_3(\eta)$ and $g_4(\eta)$ can be determined by a matching requirement between the inner and the outer solutions behind the shock similar to that in §6. The results are

$$g_4(\eta) = \gamma G_2(\eta), \tag{A 10}$$

$$\frac{1}{u_{0*}^0} g_3(\eta) - \frac{u_{0*}^0}{2\gamma} g_4(\eta) = u_{0*}^0 G_1(\eta), \tag{A 11}$$

$$C_4 + \frac{1}{u_{0*}^{02}} \int_0^1 g_3(\eta)\, \mathrm{d}\eta = p_{0*}^0 h_0, \tag{A 12}$$

where the functions $G_1(\eta)$, $G_2(\eta)$ and the constant h_0 are given by (B 28), (B 29) and (B 30) of Appendix B. Equations (A 10)–(A 12) can be used to determine $g_4(\eta)$, $g_3(\eta)$ and C_4 successively.

Appendix B. Solution for the functions U_3, V_3, R_3 and P_3 in the expansions (51*a*)–(51*d*) for the inner solution behind the shock

The linear governing equations for U_3, V_3, R_3 and P_3 are similar to (52), with the same coefficients for the homogeneous part but rather lengthy expressions for the non-homogeneous part. Only the results are given below for brevity. They are

$$U_3 = (a_{11} + a_{12}\eta^2)\,\xi^1 + (\delta_1 - f_0\theta_2)\,\xi^1\sigma_1(\zeta,\eta) - \frac{u_{0*}^0 \delta_0}{\gamma M_0^2}\,\xi^{12}\sigma_2(\zeta,\eta) + u_{0*}^0 \left\{ G_1(\eta) - \frac{1}{\gamma M_0^2} M(\zeta,\eta) \right\}, \tag{B 1}$$

$$V_3 = a_{21}(\eta - \eta^3) + \theta_1 \tau_0(\zeta,\eta) + (\delta_2 - \beta_0\theta_2)\,\xi^1\tau_1(\zeta,\eta) - \frac{\beta_0 u_{0*}^0 \delta_0}{\gamma f_0 M_0^2}\,\xi^{12}\tau_2(\zeta,\eta) - \frac{\beta_0 u_{0*}^0}{\gamma f_0 M_0^2} N(\zeta,\eta), \tag{B 2}$$

$$R_3 = (a_{31} + a_{32}\eta^2)\,\xi^1 + \left(\delta_3 + \frac{M_0^2\theta_2}{u_{0*}^{02}} \right) \xi^1\sigma_1(\zeta,\eta) + \frac{r_{0*}^0 \delta_0}{\gamma}\,\xi^{12}\sigma_2(\zeta,\eta) + r_{0*}^0 \left\{ G_2(\eta) + \frac{1}{\gamma} M(\zeta,\eta) \right\}, \tag{B 3}$$

$$P_3 = (a_{41} + a_{42}\eta^2)\,\xi^1 + \theta_2\,\xi^1\sigma_1(\zeta,\eta) + \delta_0 p_{0*}^0\,\xi^{12}\sigma_2(\zeta,\eta) + p_{0*}^0 M(\zeta,\eta), \tag{B 4}$$

where

$$a_{11} = \frac{u_{0*}^{0\prime}}{\beta_0^2}\left\{(1+M_0^2)\,\alpha_1 + M_0^2\,\alpha_2 - \frac{1+M_0^2+(\gamma-1)\,M_0^4}{\gamma M_0^2}\,(\alpha_3+\tfrac{1}{3}\beta_3)\right\}$$
$$-\tfrac{1}{6}f_0(u_0^0 f')''_* + \frac{2-2M_0^2-\gamma M_0^4}{6\beta_0^4} f_0'(u_0^0 f')'_*, \quad \text{(B 5)}$$

$$a_{12} = -u_{0*}^{0\prime}(\beta_1+\beta_2) - f_0'(u_0^0 f')'_* + \tfrac{1}{2}f_0(u_0^0 f')''_*, \quad \text{(B 6)}$$

$$a_{21} = -\tfrac{1}{3}u_{0*}^{0\prime}(2\beta_1+\beta_2) + \frac{M_0^4+2M_0^2-2}{6\beta_0^2} f_0'(u_0^0 f')'_* + \tfrac{1}{6}f_0\beta_0^2(u_0^0 f')''_*, \quad \text{(B 7)}$$

$$a_{31} = \frac{u_{0*}^{0\prime}}{f_0\beta_0^2 u_{0*}^{02}}\left\{-2M_0^2(\alpha_1+\tfrac{1}{3}\beta_1) - M_0^2(2-M_0^2)\,\alpha_2 - \tfrac{1}{3}M_0^2\beta_2\right.$$
$$\left. + \frac{1}{\gamma}\left[2+(\gamma-2)\,M_0^2+M_0^4\right](\alpha_3+\tfrac{1}{3}\beta_3)\right\}$$
$$+\frac{M_0^2}{6u_{0*}^{02}}(u_0^0 f')''_* + \frac{M_0^2(\gamma M_0^4+2M_0^2-2)}{6f_0\beta_0^4 u_{0*}^{02}} f_0'(u_0^0 f')'_*, \quad \text{(B 8)}$$

$$a_{32} = -\frac{M_0^2}{f u_{0*}^{02}} u_{0*}^{0\prime} + \frac{\gamma M_0^4 f_0'}{2f_0\beta_0^2 u_{0*}^{02}}(u_0^0 f')'_* - \frac{M_0^2}{2u_{0*}^{02}}(u_0^0 f')''_*, \quad \text{(B 9)}$$

$$a_{41} = \frac{u_{0*}^{0\prime}}{f_0\beta_0^2}\,2(\alpha_1+\tfrac{1}{3}\beta_1) + (\alpha_2+\tfrac{1}{3}\beta_2) + \frac{2-M_0^2+\gamma M_0^4}{\gamma M_0^2}(\alpha_3+\tfrac{1}{3}\beta_3)$$
$$+\tfrac{1}{6}(u_0^0 f')''_* + \frac{\gamma M_0^4+2M_0^2-2}{6f_0\beta_0^4} f_0'(u_0^0 f')'_*, \quad \text{(B 10)}$$

$$a_{42} = -\tfrac{1}{2}(u_0^0 f')''_*, \quad \zeta = \frac{\xi^1}{\beta_0 f_0}, \quad \text{(B 11), (B 12)}$$

$$\delta_0 = -\frac{\pi[2-2M_0^2+(\gamma+1)\,M_0^4]}{4f_0\beta_0^3 u_{0*}^0}\beta_3 u_{0*}^{0\prime}, \quad \text{(B 13)}$$

$$\delta_1 = \frac{\beta_0^2}{\gamma M_0^2}\beta_3 u_{0*}^{0\prime}, \quad \delta_2 = \frac{1+\frac{1}{2}(\gamma-1)\,M_0^2}{\gamma\beta_0 f_0}\beta_3 u_{0*}^{0\prime}, \quad \text{(B 14), (B 15)}$$

$$\delta_3 = \frac{(\gamma-1)\,M_0^2}{\gamma f_0 u_{0*}^{02}}\beta_3 u_{0*}^{0\prime}, \quad \text{(B 16)}$$

$$\theta_1 = -\frac{f_0[4-(3-\gamma)\,M_0^2]}{2\pi\gamma}\beta_3 u_{0*}^{0\prime}, \quad \text{(B 17)}$$

$$\theta_2 = \frac{8-8M_0^2+3(\gamma+1)\,M_0^4}{4\gamma M_0^2\beta_0^2 f_0}\beta_3 u_{0*}^{0\prime}, \quad \text{(B 18)}$$

$$\sigma_1(\zeta,\eta) = \sum_{n=0}^{\infty} b_n\,\mathrm{e}^{-n\pi\zeta}\cos n\pi\eta, \quad \text{(B 19)}$$

$$\sigma_2(\zeta,\eta) = \sum_{n=1}^{\infty} n b_n\,\mathrm{e}^{-n\pi\zeta}\cos n\pi\eta, \quad \text{(B 20)}$$

$$\tau_0(\zeta,\eta) = \sum_{n=1}^{\infty} \frac{b_n}{n}\,\mathrm{e}^{-n\pi\zeta}\sin n\pi\eta, \quad \text{(B 21)}$$

$$\tau_1(\zeta,\eta) = \sum_{n=1}^{\infty} b_n \, \mathrm{e}^{-n\pi\zeta} \sin n\pi\eta, \tag{B 22}$$

$$\tau_2(\zeta,\eta) = \sum_{n=1}^{\infty} n b_n \, \mathrm{e}^{-n\pi\zeta} \sin n\pi\eta, \tag{B 23}$$

with
$$b_0 = \tfrac{1}{3}, \quad b_n = \frac{4(-1)^n}{\pi^2 n^2} \quad (n = 1, 2, 3, \ldots). \tag{B 24}$$

The terms containing $G_1(\eta)$, $G_2(\eta)$, $M(\zeta,\eta)$ and $N(\zeta,\eta)$ in (B 1)–(B 4) are the general solution due to the homogeneous part of the governing equations, with $M(\zeta,\eta)$ and $N(\zeta,\eta)$ being of the form

$$\left.\begin{aligned} M(\zeta,\eta) &= \sum_{n=0}^{\infty} h_n \, \mathrm{e}^{-n\pi\zeta} \cos n\pi\eta, \\ N(\zeta,\eta) &= \sum_{n=1}^{\infty} h_n \, \mathrm{e}^{-n\pi\zeta} \sin n\pi\eta. \end{aligned}\right\} \tag{B 25}$$

The arbitrary functions $G_1(\eta)$, $G_2(\eta)$ and the arbitrary constants h_n $(n = 0, 1, 2, \ldots)$ can be determined by the shock conditions. If we define

$$\omega(\eta) = \nu_0 + \sum_{n=1}^{\infty} \nu_n \cos n\pi\eta \tag{B 26}$$

with
$$\nu_0 = \sum_{n=1}^{\infty} (-1)^n \frac{b_n}{n} = \frac{2}{3}, \quad \nu_n = \frac{b_n}{n} \quad (n = 1, 2, 3, \ldots), \tag{B 27}$$

we have

$$G_1(\eta) = \frac{\beta_0\beta_3 f_0 u_{0*}^{\mathrm{o}}}{\pi\gamma M_0^2 (u_{0*} - u_{0*}^{\mathrm{o}})} \left\{ \frac{\nu_0}{\gamma M_0^2} \left(\frac{p_{0*}'}{p_{0*}} + k_p \frac{u_{0*}'}{u_{0*}} - \frac{p_{0*}^{\mathrm{o}\prime}}{p_{0*}^{\mathrm{o}}} \right) \right.$$
$$\left. + \left[\frac{1}{\gamma M_0^2} \left(\frac{p_{0*}'}{p_{0*}} + k_p \frac{u_{0*}'}{u_{0*}} - \frac{p_{0*}^{\mathrm{o}\prime}}{p_{0*}^{\mathrm{o}}} \right) - \frac{u_{0*}'}{u_{0*}} - \frac{u_{0*}^{\mathrm{o}\prime}}{u_{0*}^{\mathrm{o}}} \right] \omega(\eta) \right\}, \tag{B 28}$$

$$G_2(\eta) = \frac{\beta_0\beta_3 f_0 u_{0*}^{\mathrm{o}}}{\pi\gamma^2 M_0^2 (u_{0*} - u_{0*}^{\mathrm{o}})} \left\{ \nu_0 \left(\frac{p_{0*}^{\mathrm{o}\prime}}{p_{0*}^{\mathrm{o}}} - \frac{p_{0*}'}{p_{0*}} - k_p \frac{u_{0*}'}{u_{0*}} \right) \right.$$
$$\left. - \left[\frac{p_{0*}'}{p_{0*}} + k_p \frac{u_{0*}'}{u_{0*}} - \frac{p_{0*}^{\mathrm{o}\prime}}{p_{0*}^{\mathrm{o}}} + \gamma \left(\frac{r_{0*}^{\mathrm{o}\prime}}{r_{0*}^{\mathrm{o}}} - \frac{2u_{0*}'}{u_{0*}} - \frac{r_{0*}'}{r_{0*}} \right) \right] \omega(\eta) \right\}, \tag{B 29}$$

$$h_n = \frac{\beta_0\beta_3 f_0 u_{0*}^{\mathrm{o}}}{\pi\gamma M_0^2 (u_{0*} - u_{0*}^{\mathrm{o}})} \left(\frac{p_{0*}'}{p_{0*}} + k_p \frac{u_{0*}'}{u_{0*}} - \frac{p_{0*}^{\mathrm{o}\prime}}{p_{0*}^{\mathrm{o}}} \right) \nu_n \quad (n = 0, 1, 2, \ldots). \tag{B 30}$$

Also, the function $k(\eta)$ in the shock-shape equation (74) can be found as

$$k(\eta) = \tfrac{1}{8} f_0 f_0' (f_0 f_0'' + 3 f_0'^2)(\eta^4 - 1) - \tfrac{1}{4} f_0 f_0' (f_0 f_0'' + f_0'^2)(\eta^2 - 1)$$
$$+ \frac{f_0^2}{4(u_{0*} - u_{0*}^{\mathrm{o}})} \left\{ u_{0*} \left[\tfrac{1}{6}\beta_0^2 f_0 f_0''' + f_0 f_0'' \left(\tfrac{1}{2}\beta_0^2 - 2 + \frac{2\beta_0^2 u_{0*}^2}{(\gamma+1)(1 - u_{0*}^2)^2} \right) \right] \right.$$
$$\left. - a_{21} + \tfrac{1}{3}\theta_1 - \frac{\beta_0^2 \beta_3 u_{0*}^{\mathrm{o}2}}{3\pi\gamma^2 M_0^4 (u_{0*} - u_{0*}^{\mathrm{o}})} \left(\frac{p_{0*}'}{p_{0*}} + k_p \frac{u_{0*}'}{u_{0*}} - \frac{p_{0*}^{\mathrm{o}\prime}}{p_{0*}^{\mathrm{o}}} \right) \right\} (\eta^2 - 1). \tag{B 31}$$

REFERENCES

ADAMSON, T. C., MESSITER, A. F. & LIOU, M. S. 1978 *AIAA J.* **16**, 1240–1247.
CHAN, S. K. & ADAMSON, T. C. 1978 *AIAA J.* **16**, 377–384.
LIN, C. Q. & SHEN, S. F. 1981 *AIAA J.* **19**, 1494–1496.
LIN, C. Q. & SHEN, S. F. 1982 *AIAA Paper* AIAA-82-0160.
MESSITER, A. F. & ADAMSON, T. C. 1975 *J. Fluid Mech.* **69**, 97–108.
RICHEY, G. K. & ADAMSON, T. C. 1976 *AIAA J.* **14**, 1054–1061.